Investigation of Breakthrough Curves of Citric Acid Adsorption

doi: 10.15255/CABEQ.2013.1872
Original scientific paper
Received: October 7, 2013
Accepted: July 28, 2014

S. A. Ghorbanian, M. Davoudinejad, A. Khakpay, and S. Radpour
Chemical engineering department, Faculty of Engineering,
University of Tehran, P.O.Box 11365/4563, Tehran, I.R. Iran

In this paper, experimental breakthrough curves for citric acid adsorption from aqueous solution onto ion-exchange resin at 20, 35, 55 °C have been obtained by some weak and strong basic anionic resins, such as IRA-92, IRA-93, IRA-420 and IRA-458. The results show that amberlite IRA-93 has good performance and is one of the best resins in the process of citric acid recovery from aqueous solution. Also, the temperature effect study shows that an increase in temperature causes an increase in diffusion coefficient of particles, but the saturation capacity of resin decreases. To achieve an appropriate model, three mathematical models were analyzed to predict system properties based on statistical tests, and finally, the appropriate model was determined. To examine model capability, mathematical equations have been implemented in various breakthrough curve data obtained by other investigators, and the results show appropriate conformity.

Key words:
adsorption, breakthrough curves, modeling, citric acid

Introduction

Citric acid is the most widely used organic acid in the field of foods and beverages as an acidulant as well as in pharmaceutical and chemical products. Generally, surface or submerged fungal fermentation mainly with *aspergillus niger* is utilized for citric acid production. However, the submerged fermentation method is the most used method for citric acid production.[1,2] The method of calcium salt precipitation is an established process for citric acid purification. a series of precipitation and isolation reactions using $Ca(OH)_2$ and H_2SO_4 can be exploited for citric acid separation from fermentation broths.[3,4] However, this process includes several batch treatments in which huge amounts of chemical reagents and a large amount of heat are required. These negative factors have directed many investigators to find new techniques to separate or purify citric acid from fermentation broths, such as adsorption and electro-dialysis.[5,6]

Electro-dialysis as an electrochemical separation process charged the membranes electrically. For separation of ionic species from aqueous solutions, electrical potential difference is used. The electro-dialysis was used in citric acid recovery. However, the main problem is that the costs of this technique were determined to be approximately 50 % higher compared to the current industrial citric acid recovery process. The use of electro-dialysis requires the development of new processes to decrease waste formation and enhance productivity.[7]

*Corresponding author: e-mail: saeidrez@ualberta.ca

Purification of organic acids, particularly citric acid, by adsorption process has lower production costs compared to other methods. Attention has been drawn to the novel use of synthetic ion-exchange resins in separation and purification of organic acids.[8,9] This set of adsorbents acts selectively and other components of solution remain intact. After saturation of solid adsorbent at the end of a separation operation period, it is recovered by elution with water, acid or base. Although the principle of organic acids separation by ion-exchange method is known, there are many details that require development and increment. Thus, it seems that Simulated Moving Bed (SMB) by using chromatography method on the base of countercurrent continuous contact between feed and adsorbent is appropriate and effective.[10,11]

SMB is a continuous chromatographic method which requires determined parameters like ion-exchange resins properties, adsorption equilibrium data, and operating characteristics of bed. One of the best methods to specify and optimize operating parameter is to prepare a fitting mathematical model from actual processes. Generally in such models, mass transfer in liquid layer outside the resin particles is negligible. The general ion-exchange reaction of resin is presented in eq. 1.[12–14]

$$\text{R-N} + \text{CH}_n \rightleftarrows \text{R-NH}^+\text{CH}^-_{n-1} \qquad (1)$$

For acids with more than one carboxyl group, and for R-N in eq. 1, base resins are appropriate.[15]

Estimation of breakthrough curves is required for successful design of an adsorption column. For a fixed-bed randomly-packed adsorption column, which is fed from the top of the bed at a constant flow rate, by an aqueous solution containing an organic pollutant, the mass transfer balance equation for predicting fixed-bed dynamics is:[16–19]

$$\varepsilon\frac{\partial C}{\partial t}+U_0\left(\frac{\partial C}{\partial Z}\right)+(1-\varepsilon)\left(\frac{\partial q}{\partial t}\right)=D_p\left(\frac{\partial^2 C}{\partial Z^2}\right) \quad (2)$$

where ε is the void fraction in the column, C is concentration, t is time, U_0 is superficial velocity, Z is column depth, q is concentration in the stationary phase, D_p is diffusivity.

The overall mass balance on the adsorbed solute is:

$$(1-\varepsilon)\left(\frac{\partial q}{\partial t}\right)=p \quad (3)$$

here p is the adsorption rate.

The initial and boundary conditions for eq. 2 are:

$$C=C_0 \qquad t=0,\ Z=0 \quad (4)$$

$$D_L\frac{\partial C}{\partial Z}=-U_0\left(C_0-C\right) \qquad t>0,\ Z=0 \quad (5)$$

$$\left(\frac{\partial C}{\partial Z}\right)=0 \qquad t>0,\ Z=L \quad (6)$$

where C_0 is initial concentration, and D_L is axial dispersion coefficient.

The following assumptions are associated with eq. 2:

- No chemical reactions take place in the column.
- Radial and axial dispersions are negligible.
- The flow pattern is the ideal plug flow.
- The temperature in the column is constant with time.
- The column flow rate is constant and unchanged with the column position.[16–19]

In this study, experimental breakthrough curves for citric acid adsorption from aqueous solution onto ion-exchange resin at different temperatures have been obtained. Several mathematical models have been developed and analyzed to predict system properties based on experimental data.

Breakthrough curves

Equations heretofore offered for describing breakthrough curves are somewhat complicated expressions that can only describe ideal, symmetrical breakthrough curves, while for other possible shapes they are unable to generate acceptable results. In some cases, these equations were obtained from mass balances along with simplification assumptions[20,21] that were often offered for gas breakthrough curves, or included additional fitting parameters to better describe asymmetric (skewed) breakthrough curves, such as the Wood equation, and others are only mathematical equations that generate S-shaped curves.[22,23]

In this research work, we attempted to derive mathematical equations that could not only predict symmetrical S-shaped breakthrough curves, but also describe other curves from which they deviate. Furthermore, several models in different forms, such as fractional, polynomial, and exponential were developed and statistically analyzed. Finally, three new mathematical fitting models, two implicit and one explicit, in the following forms were developed for prediction breakthrough curves.

Implicit models

Developed implicit models are shown in eqs. 7 and 8. These equations can be divided into two categories including two- and three-parameter models. Parameters A, B, J, n, and r are fitting constant parameters that must be determined by regression of the experimental data.

$$\frac{C}{C_0}=\frac{At}{B+\left(C/C_0\right)^n} \quad (7)$$

$$\frac{C}{C_0}=\frac{J\ln(1+t)}{1+\left(C/C_0\right)^r} \quad (8)$$

where A, B, J, n and r are constants.

Explicit model

Using explicit equations because of their simple usage has preference, but often it seems difficult to develop explicit equations with a suitable simplicity that possesses enough generality. Implicit models usually have better performance for describing different experimental data curves compared to explicit models. But, implicit models require trial and error calculations in order to solve them. In this section, implicit equations were transformed to their analog explicit equations. Afterwards, an explicit equation was determined by replacing C/C_0 with t/t_F in eq. 8.

$$\frac{C}{C_0}=\frac{D'\ln(1+t)}{E'+\left(t/t_F\right)^{m'}} \quad (9)$$

where t_F is the time in which C/C_0 reaches 0.999, and D', E' and m' are constants.

Experimental

In preliminary experiments, several types of weak and strong basic anionic resins such as, IRA-92, IRA-93, IRA-420 and IRA-458 were examined, and finally amberlite IRA-93 was selected because of its high performance and compatibility in acid adsorption. Experiments were then planned to investigate temperature effect on IRA-93 adsorption capacity. The experimental apparatus consists of a glass column (ID = 1 cm, height = 20 cm) and a bed (volume = 15 cm^3). A schematic diagram of the apparatus used is depicted in Fig. 1. The volumetric flow rate of acid in adsorption and desorption is constant and equals 1.5 mL min^{-1}. Moreover, the experiments were carried out at three temperatures (20, 35, and 55 ºC) in which about 25 samples were analyzed for each temperature. The influent solution contains 20 wt. % of citric acid, and the elution process is performed by 0.2 molar sulfuric acid solution. Furthermore, the concentration of citric acid was determined by a spectrophotometer UV-VIS (Model: Cary 1E/ Cary 3E, Purchased from Varian Co.). For determination of the breakthrough curves, dynamic experiments were developed. In addition, the concentration of citric acid was determined only at the bottom of the column, and axial distribution was not considered.

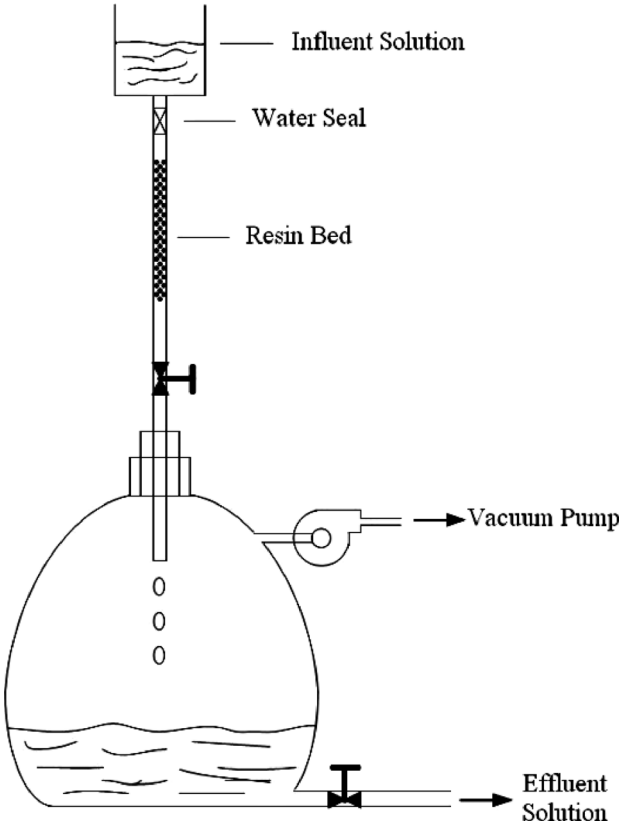

Fig. 1 – *Schematic diagram of experimental apparatus*

Results and discussion

The breakthrough curves were measured at 20, 35, and 55 ^{0}C. The results show that weak basic resins are suitable for citric acid recovery in water solutions. In addition, citric acid diffusivity and resin saturation capacity were obtained at different temperatures and the results are shown in Table 1. Diffusivities were determined using Perry's Chemical Engineering Handbook.[24] Moreover, parameter A which is multiplied by t could not properly follow up the amounts of concentration, therefore, eq. 8 correlation was developed, and the results improved clearly.

Table 1 *Diffusivities and resin saturation capacity at different temperatures*[24]

C_m (g L^{-1})	$D_p \cdot 10^{10}$ (m^2 s^{-1})	T (°C)
302.2	3.1	20
265.1	4.3	35
190.4	6.1	55

In this way, number 1 is added to the logarithmic term, which makes that available at evident point (0, 0). The constants of all models were obtained by ordinary least square method using the "Eviews software" version 3.1.[25] In Eviews software, several analyses are carried out for analyzing and fitting of data that are explained as follows:

R-squared: The *R*-squared (R^2) statistic measures the success of the regression in predicting the values of the dependent variable within the sample. The statistic will be equal to one if the regression fits perfectly.

Durbin-Watson Test: D.W. is another parameter considering the difference between real and model amount in every point known as residual. In fact, this parameter determines the relation between residual data.

In addition to R^2 and D.W., the mean relative percent error, MRPE, was utilized in order to choose the best fitting model. Furthermore, MRPE was used to compare the predicted results with the experimental data. MRPE was calculated from the following formula.

$$MRPE = \frac{1}{ND}\sum_{i=1}^{N}\left|\frac{\left(C/C_0\right)_{Exp} - \left(C/C_0\right)_{Equ}}{\left(C/C_0\right)_{Exp}}\right| \cdot 100 \quad (10)$$

where MRPE is the mean absolute percent error, ND is the number of data points, $(C/C_0)_{Exp}$ is the experimentally measured relative concentration, and $(C/C_0)_{Equ}$ is the relative concentration determined using equations.

Table 2 – *Models fitting results for citric acid data*

Models	T = 20 °C			T = 35 °C			T = 55 °C			Average MRPE
	% R^2	D.W.	MRPE	% R^2	D.W.	MRPE	% R^2	D.W.	MRPE	
Eq. 7	92.42	0.426	35.44	96.38	0.342	23.70	99.74	1.04	16.25	25.13
Eq. 8	99.91	0.471	13.01	99.88	0.460	12.19	99.83	0.266	20.62	15.27
Eq. 9	99.60	1.56	7.06	99.30	1.49	12.32	98.65	1.43	28.80	16.06

Table 2 shows the calculation results for selected models. As shown in Table 2, R^2 is greater than 0.99 except in three cases, and it is 0.999 for many cases. In addition, according to the amounts of R^2, DW, and MRPE, eqs. 8 and 9 well describe the adsorption of citric acid on the IRA-93 resin as implicit and explicit models, respectively. Furthermore, the calculation results show that performance of equations is satisfactory except eq. 7. However, eq. 8 has the best fitting results compared to other models and can predict alteration of citric acid adsorption breakthrough curves with very low MRPE. In contrast, eq. 9 has 5 % more MRPE compared to eq. 8, but it is easy to use. At first it seems that implicit equations are very difficult to use, but these models are simple for determining the unknown value of the equation. Also, they are more precise than other models for breakthrough curves. Moreover, Table 3 shows the constant estimation of eq. 9 for temperatures 20, 35 and 55 °C. Furthermore, the results of eq. 9 are plotted in Fig. 2, and this model is in conformity with the experimental data. According to Fig. 2, an increase in temperature causes an increase in adsorption of citric acid.

Table 3 – *Calculation results of the coefficients of eq. 9 at temperatures 20, 35 and 55 °C*

Models	Equation parameters	20 °C	35 °C	55 °C
Eq. 9	D'	37.42	27.32	24.41
	E'	324.60	234.98	211.68
	m'	–5.509	–7.789	–11.469

In aqueous solution, weak dispersion forces dominate interactions between organic compounds and hydrophobic surfaces. Therefore, the adsorption can be considered reversible. It is proposed that citric acid adsorption on IRA-93 contains four steps: Diffusion through the bulk liquid, film diffusion, intra-particle diffusion, and adsorption on the solid surface. Generally, the bulk liquid diffusion and adsorption steps happen quickly and, therefore, they are not rate-limiting. Intra-particle diffusion is in the pore space (i.e., pore diffusion) or along the adsorbent surface in the pores (i.e., surface diffusion).

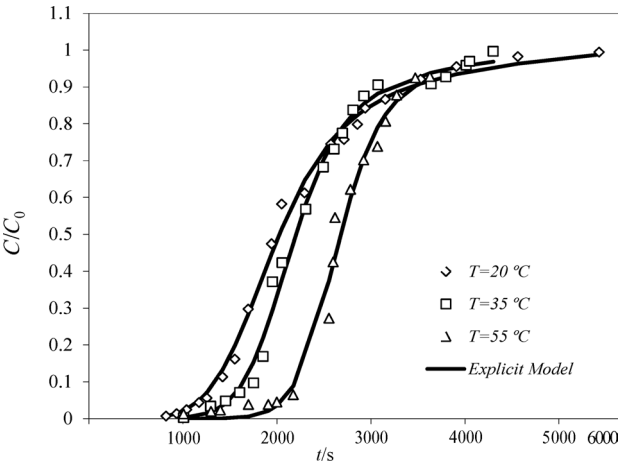

Fig. 2 – *Citric acid adsorption breakthrough curves data points fitted by equation 9 at 20, 35 and 55 °C*

Intra-particle diffusion studies investigating the adsorption of organic compounds showed that surface diffusion typically dominates over pore diffusion. Therefore, the citric acid adsorption by IRA-93 is also controlled by surface diffusion.[26,27]

To investigate the correlations accuracy (eqs. 7 to 9), the models were compared with the breakthrough curves data of Lu *et al.* (adsorption of Pb^{2+} in a fixed bed of ETS-10 adsorbent), Gonzalez *et al.* (adsorption of Cr(III) from aqueous solution onto Agave lechuguilla biomass), Grande *et al.* (adsorption of propylene in zeolite 4A), Ahmaruzzaman *et al.* (adsorption of phenol from wastewater by different adsorbents), Pan *et al.* (adsorption of phenol onto resin NDA-100), and Malkoc *et al.* (adsorption of Cr(VI) onto waste acorn of *Quercus ithaburensis*).[28–33]

In detail, 18 breakthrough curves were utilized in order to determine reliability of model. From this, eqs. 7 to 9 were fitted to these breakthrough curves and the results are shown in Table 4. According to Table 4, MRPE (a mean value) for implicit models (eqs. 7 and 8) are in good agreement with

Table 4 – *Models fitting results for selected breakthrough curves data*

Models	Eq. 7	Eq. 8	Eq. 9
Averaged MRPE	11.73	9.92	14.20

experimental breakthrough curves. Furthermore, MRPE for eq. 9 is acceptable because of its explicit form. Moreover, the amounts of R^2 are more than 0.99 for all of the adsorbates, even in the experiments with S-shape of the curve. Similar to our breakthrough curves, equation 8 best fitted with experimental data and the average MRPE was 9.92.

Breakthrough curves that were fitted based on eq. 9 are shown in Figs. 3 to 8. The calculation results for constants of eq. 9 are presented in Table 5. Although, in most cases the curve deviates from the S shape and average MRPE in all cases is 14.20 % and correlation coefficients (R^2) are higher than 0.984 for all cases. Consequently, although eq. 9 is not as effective as eq. 8 to fit experimental data, but eq. 9 is simple to use.

Among developed implicit equation models, eq. 8 showed the best conformity with experimental data. Proper fitting indicated by R^2 amounts near to 1.0 (0.999) and low average MRPE over uneven breakthrough curves of citric acid is 15.27. Furthermore, for the selected breakthrough curves from various chemical systems it is 9.92. The explicit model presented by eq. 9 is not as effective as implicit models to fit experimental data, but this equation is easy to use. Although in most cases, the curve deviates from "S" shape, but average MRPE over uneven

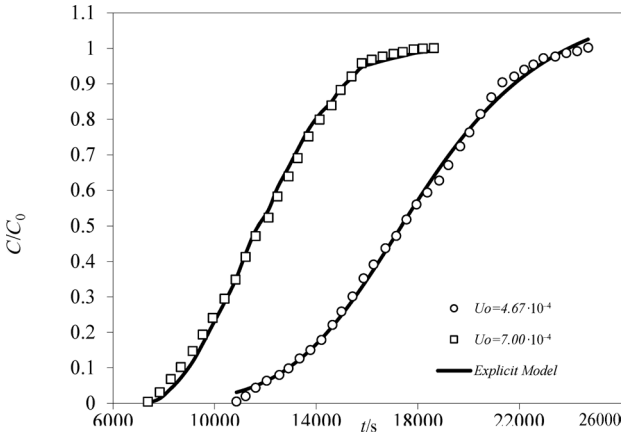

Fig. 3 – *Breakthrough curves of Pb^{2+} adsorption onto ETS-10 at different superficial velocity*[28]

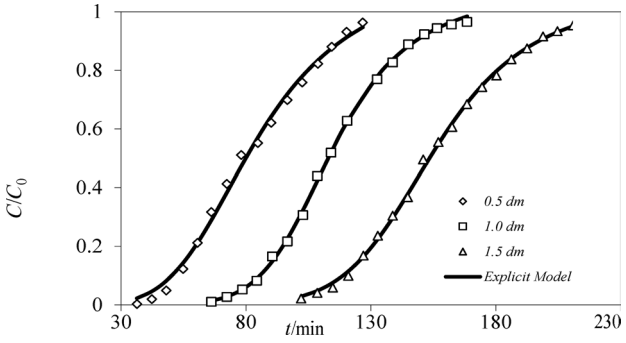

Fig. 4 – *Adsorption breakthrough curves of Cr(VI) onto waste acorn of Quercus ithaburensis*[29]

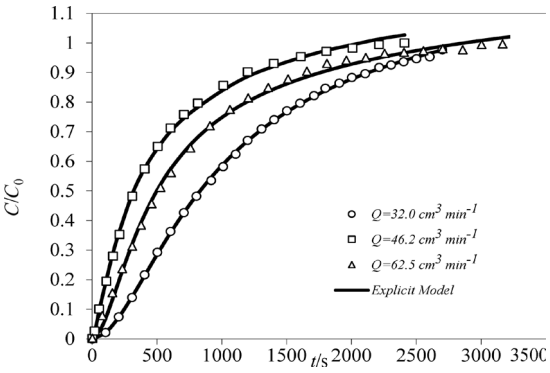

Fig. 5 – *Adsorption breakthrough curves of phenol onto resin NDA-100 in different initial concentration*[30]

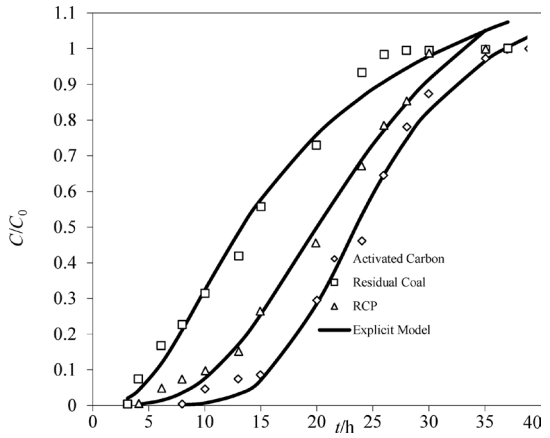

Fig. 6 – *Adsorption breakthrough curves of Phenol onto different adsorbent*[31]

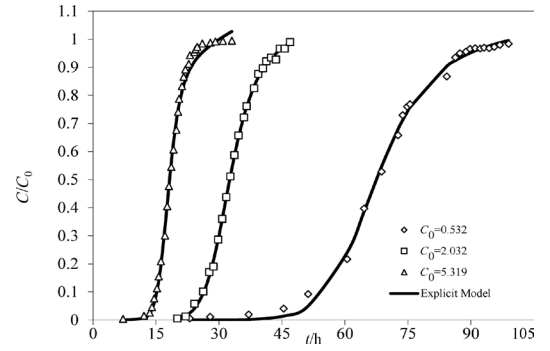

Fig. 7 – *Breakthrough curves of phenol adsorption onto resin NDA-100 in different initial concentration*[32]

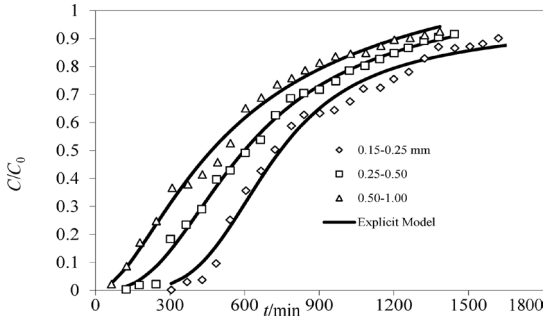

Fig. 8 – Breakthrough curves of Cr(III) adsorption onto lechuguilla biomass at different bed lengths[33]

Table 5 – *Fitting different breakthrough curves based on eq. 9, related statistical tests and MRPE*

Breakthrough curve	Case		D'	E'	m'	R^2 %	D.W.	MRPE
Adsorption of Pb^{2+} onto ETS-10 adsorbent	U_0 (m s^{-1})	$4.67 \cdot 10^{-4}$	1.155	10.391	–7.074	99.79	0.300	19.89
		$7.00 \cdot 10^{-4}$	2.412	22.073	–6.895	99.79	0.359	27.97
Adsorption of Cr(VI) onto waste acorn of *Quercus ithaburensis*	Particle size (mm)	0.15–0.25	6.756	56.061	–4.296	98.52	0.533	17.89
		0.25–0.50	1.917	14.344	–2.636	99.54	1.98	20.00
		0.50–1.00	1.58	7.881	–1.699	99.06	0.834	5.06
Adsorption of propylene onto zeolite 4A	Q (cm^3 min^{-1})	32.0	1.385	10.023	–1.678	99.97	0.862	0.77
		46.2	3.822	28.073	–1.361	99.87	0.506	9.39
		62.5	4.315	33.120	–1.596	99.76	0.390	7.39
Adsorption of phenols from wastewater	Adsorbent	Activated carbon	5.501	18.613	–5.527	99.24	1.33	17.63
		RCP	1.820	5.200	–3.151	99.17	2.08	19.01
		Residual coal	5.351	17.116	–2.380	98.41	0.838	38.74
Adsorption of phenol onto resin NDA-100	C_0 (mmol L^{-1})	0.532	17.640	80.446	–10.763	99.76	1.68	15.09
		2.032	19.331	74.555	–10.593	99.93	2.39	4.03
		5.319	7543.53	25887.4	–12.525	99.34	0.235	9.61
Adsorption of Cr(III) onto Agave lechuguilla biomass	Bed length (dm)	0.5	2.230	10.296	–4.585	99.52	0.659	17.86
		1.0	5.603	28.144	–7.870	99.93	2.60	4.70
		1.5	4.090	21.766	–8.561	99.89	1.56	6.29

breakthrough curves of citric acid is 16.06 and for selected breakthrough curves from various chemical systems it is 14.20. The correlation coefficients (R^2) are greater than 0.984 in all cases.

Fig. 9 presents the results of the sensitivity analysis performed for equation 9. According to Fig. 9, eq. 9 shows a good performance to a 20 percent change in time (see slopes of the curves).

Furthermore, our data has been evaluated using other researchers' models. Three different models

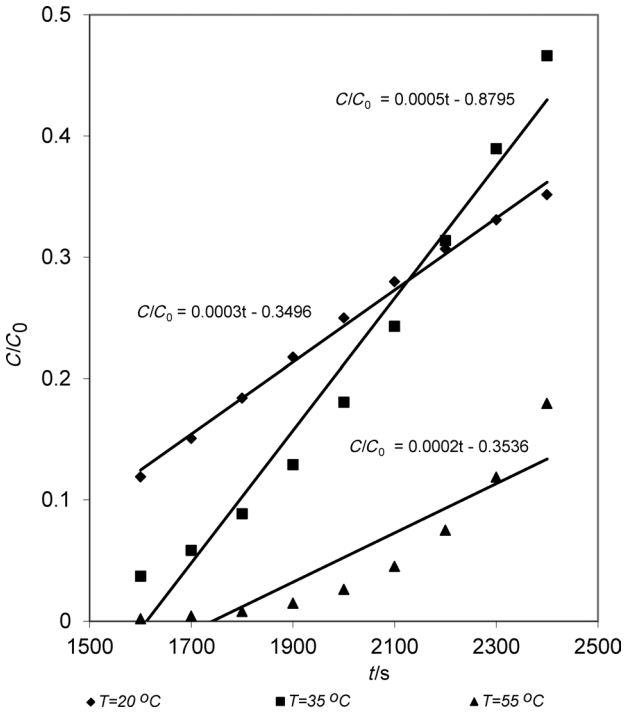

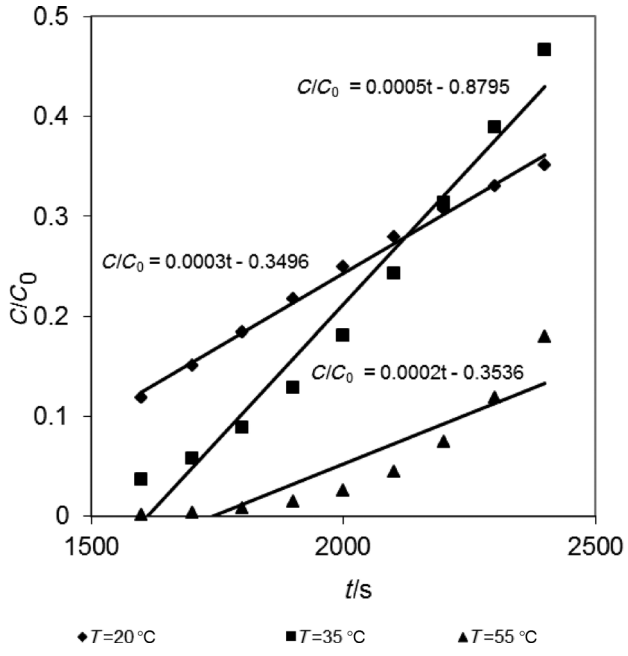

Fig. 9 – *Sensitivity analysis for eq. 9*

Table 6 – *Comparison of different models and eq. 9*

Model's name	Model	Average MRPE
Eq. 9	$\frac{C}{C_0}=\frac{D'\ln(1+t)}{E'+\left(t/t_F\right)^{m'}}$	16.06
Adams-Bohart	$\ln\frac{C}{C_0}=k_{AB}C_0t-k_{AB}N_0\frac{Z}{U_0}$	114.52
Yoon-Nelson	$\ln\frac{C}{C_0-C}=k_{YN}t-\tau k_{YN}$	90.82
Chern	$t=\tau+\frac{\rho N_1}{\varepsilon K_L a C_0}\left[\ln\left(\frac{2C}{C_0}\right)+\frac{1}{1+KC_0}\ln\left(\frac{1}{2\left(1-\frac{C}{C_0}\right)}\right)\right]$	18.70

derived by Adams-Bohart, Yoon-Nelson, and Chern have been chosen in order to assess our model.[18,19] The results are shown in Table 6. According to Table 6, we improved the MRPE around 12.12 % using eq. 9. Moreover, eq. 9 is easy to use.

Conclusion

An experimental investigation was performed to obtain the adsorption breakthrough curves for citric acid at 20, 35, and 55 ^{0}C. Amberlite IRA-93 resin was used as adsorbent. Implicit and explicit models were utilized in order to correlate breakthrough curves. The results were analyzed and summarized as follows.

Weak basic resins are more appropriate for adsorption of citric acid onto an adsorbent than strong basic resins because of their higher mechanical strength and low cost. In addition, adsorbate diffusivity in resin increases as a result of temperature increase. Therefore, it could be suggested that low and high temperatures are inappropriate conditions for the adsorption process, whereas a middle temperature could be recommended as process design based on low diffusivity at low temperatures and resin degradation at high temperature.

Because of their structure, implicit mathematical models have good flexibility for describing various breakthrough curves with different steepness and shapes, even for unusual S-shaped type, and can also predict alteration of various adsorption breakthrough curves, but the explicit model generates smooth S-shaped curves. As a result, logarithmic models show better conformity with experimental data compared to non-logarithmic corresponding models. Since the numerical values of time are much greater than the concentration ratio, taking the logarithm of time reduces its amount and propriety arises in the equation, thus, logarithmic models give better results which are very obvious.

To probe the accuracy of the models, our models were compared with other researchers' experimental data. Totally, 18 breakthrough curves have been investigated. The results show that our models are capable of describing breakthrough curves with a wide range of data. Furthermore, we compared our model with Adams-Borhat, Yoon-Nelson, and Chern's models, and the results were in satisfactory agreement.

Nomenclature

$(C/C_0)_{Equ}$ – Relative concentration determined using equations
$(C/C_0)_{Exp}$ – Experimentally measured relative concentration
A – Equation constant parameter
a – Mass-transfer area per unit volume of the bed, m^{-1}
B – Equation constant parameter
C – Concentration, kg m^{-3}
C/C_0 – Relative concentration
C_0 – Initial concentration, kg m^{-3}
C_m – Saturation capacity, kg m^{-3}
D.W. – Durbin-Watson statistic
D' – Equation constant parameter
D_L – Axial dispersion coefficient, m^2 s^{-1}
D_P – Diffusivity, m^2 s^{-1}
E' – Equation constant parameter
J – Equation constant parameter
K – Langmuir model parameter, m^3 mol^{-1}
k_{AB} – Constant in the Adams–Bohart model, kg^{-1} s^{-1}
K_L – Overall liquid-phase mass-transfer coefficient, m s^{-1}
k_{YN} – Constant in the Yoon and Nelson model, s^{-1}

m' – Equation constant parameter
MRPE – Mean Absolute Percent Error
ND – Number of data points
N – Equation constant parameter
N_0 – Saturation concentration in the Adams–Bohart model, kg^{-1}
N_1 – Langmuir model parameter, $m^3\ mol^{-1}$
P – Adsorption rate, mol $s^{-1}\ kg^{-1}$ dry resin
q – Concentration in the stationary phase, mol $s^{-1}\ kg^{-1}$ dry resin
Q – Volumetric flow rate, $cm^3\ min^{-1}$
R – Equation constant parameter
R^2 – Correlation coefficient
SBM – Simulating Moving Bed
t – Time, s, min, or h
T – Temperature, °C
t_F – Time in which C/C_0 reaches 0.999
U_0 – Superficial velocity, m s^{-1}
Z – Column depth, m

Greek letters

ε – Void fraction in column
ρ – Bed density, kg m^{-3}
τ – Half time at $C/C_0 = 0.5$, s

References

1. *Cambier, P.,* Clays and Clay Minerals **39** (4) (1991) 369. http://dx.doi.org/10.1346/CCMN.1991.0390405
2. *Cambier, P.,* Clays and Clay Minerals **39** (2) (1991) 158. http://dx.doi.org/10.1346/CCMN.1991.0390207
3. *Cheng, T., Jiang, Y., Zhang, Y., Liu, S.,* Carbon **42** (2004) 3081. http://dx.doi.org/10.1016/j.carbon.2004.07.021
4. *Ekpete, O. A, Horsfall, M. J., Spiff, A. I.,* Australian J. Basic App. Sc. **5** (11) (2011) 1149.
5. *Mozammel, M., Sadrnezhaad, S. K., Badami, E., Ahmadi, E.,* Hydrometallurgy **85** (2007) 17. http://dx.doi.org/10.1016/j.hydromet.2006.07.003
6. *Zeinali, F., Ghoreyshi, A. A., Najafpour, G. D.,* Middle-East J. Sci. Res. **5** (4) (2010) 191.
7. *Soccol, C. R., Vandenberghe, L. P. S., Rodrigues, C., Pandey, A.,* Food Tech. Biotech. **44** (2) (2006) 141.
8. *Kulprathipanja, S., Oroskar, A., Preignitz, J.,* US patent 4851573, (1989).
9. *Cao, X., Yun, H., Koo, Y.,* Biochem. Eng. J. **11** (2002) 189. http://dx.doi.org/10.1016/S1369–703X(02)00024–4
10. *Abollino, O., Aceto, M., Malandrino, M., Sarzanini, C., Mentasti, E.,* Water Res. **37** (2003) 1619. http://dx.doi.org/10.1016/S0043–1354(02)00524–9
11. *Oh, M., Tshabalala, M. A.*, Bioresource Tech. **2** (1) (2007) 66.
12. *Takatsuji, W., Yoshida, H.*, Sep. Sci. Tech. **29** (1994) 1473. http://dx.doi.org/10.1080/01496399408003032
13. *Gluszes, P., Jamroz, T., Sencio, B., Ledakowicz, S.*, Bioprocess and Biosystem Eng. **26** (2004) 185. http://dx.doi.org/10.1007/s00449–003–0348–7
14. *Mokrini, A., Ousse, D., Esplugas, S.*, Water Sci. Tech. **35** (1997) 95. http://dx.doi.org/10.1016/S0273–1223(97)00014–0
15. *Misak, N. Z.*, Reactive Fun. Polymers, **43** (2000) 153. http://dx.doi.org/10.1016/S1381–5148(99)00046–2
16. *Murillo, R., Garcia, T., Aylon, E., Callen, M. S., Navarro, M. V., Lopez, J. M., Mastral, A. M*, Carbon **42** (2004) 2009. http://dx.doi.org/10.1016/j.carbon.2004.04.001
17. *Ghorai, S., Pant, K. K.*, Chem. Eng. J. **98** (2004) 165. http://dx.doi.org/10.1016/j.cej.2003.07.003
18. *Chern, J. M., Chien, Y. W.*, Water Res. **36** (2002) 647. http://dx.doi.org/10.1016/S0043–1354(01)00258–5
19. *Aksu, Z., Gönen, F.*, Process Biochem. **39** (2004) 599. http://dx.doi.org/10.1016/S0032–9592(03)00132–8
20. *Kodama, A.*, J. Chem. Eng. Japan **43** (2010) 901. http://dx.doi.org/10.1252/jcej.10we148
21. *LeVan, M. D., Carta, G., Yon, C. M.*, Perry's Chemical Engineers Handbook, 6th edition, New York, 1997.
22. *Wood, G.*, ***J. Int.*** Soc. Respiratory ***Prot.***, **10** (4) (1993) 5.
23. *Christiano, C., Deovaldo, M., Seleude, W., Marcio, G. B.*, Bioresource Tech. **98** (2007) 886. http://dx.doi.org/10.1016/j.biortech.2006.03.024
24. *Green, D. W., Perry, R. H.*, Perry's Chemical Engineers Handbook, 8th edition, New York, 2008.
25. Quantitative Micro Software LLC., EViews 4 User's Guide, ISBN 1–880411–28–8, 2002.
26. *Badruzzaman, M., Westerhoff, P., Knappe, D. R. U.*, Water Res. **38** (2004) 4002. http://dx.doi.org/10.1016/j.watres.2004.07.007
27. *Sperlich, A., Werner, A., Genz, A., Amy, G., Worch, E., Jekel, M.*, Water Res. **39** (2005) 1190. http://dx.doi.org/10.1016/j.watres.2004.12.032
28. *Lu, L., Zhang, Y., Wang, K., Ray, A. K., Zhao, X. S.*, J. Colloid Interface Sci. **325** (1) (2008) 57. http://dx.doi.org/10.1016/j.jcis.2008.04.067
29. *Gonzalez, J. R., Walton, J. C.*, J. Hazardous Mat. **161** (1) (2009) 360. http://dx.doi.org/10.1016/j.jhazmat.2008.03.102
30. *Grande C. A., Rodrigues, A. E.*, Chem. Eng. Res. Des. **82** (12) (2004) 1604. http://dx.doi.org/10.1205/cerd.82.12.1604.58029
31. *Ahmaruzzaman, M., Sharma, D. K.*, J. Colloid Interface Sc. **287** (2005) 14. http://dx.doi.org/10.1016/j.jcis.2005.01.075
32. *Pan, B. C., Meng, F. W.*, J. Hazardous Mat. **124** (2005) 74. http://dx.doi.org/10.1016/j.jhazmat.2005.03.052
33. *Malkoc, E., Nuhoglu, Y., Abali, Y.*, Chem. Eng. J. **119** (1) (2006) 61. http://dx.doi.org/10.1016/j.cej.2006.01.019